Detailed Characterization of Vacuum Chamber Surface Properties Using Measurements of the Time Dependence of Electron Cloud Development

Jim Crittenden

Cornell Laboratory for Accelerator-Based Sciences and Education

CESRTA Advisory Committee

29 August 2012

EC Buildup Detectors at CESRTA

L3 Electron cloud experimental region

PEP-II EC Hardware:
Chicane, SEY station
Four time-resolved RFA's
Drift and quadrupole diagnostic chambers

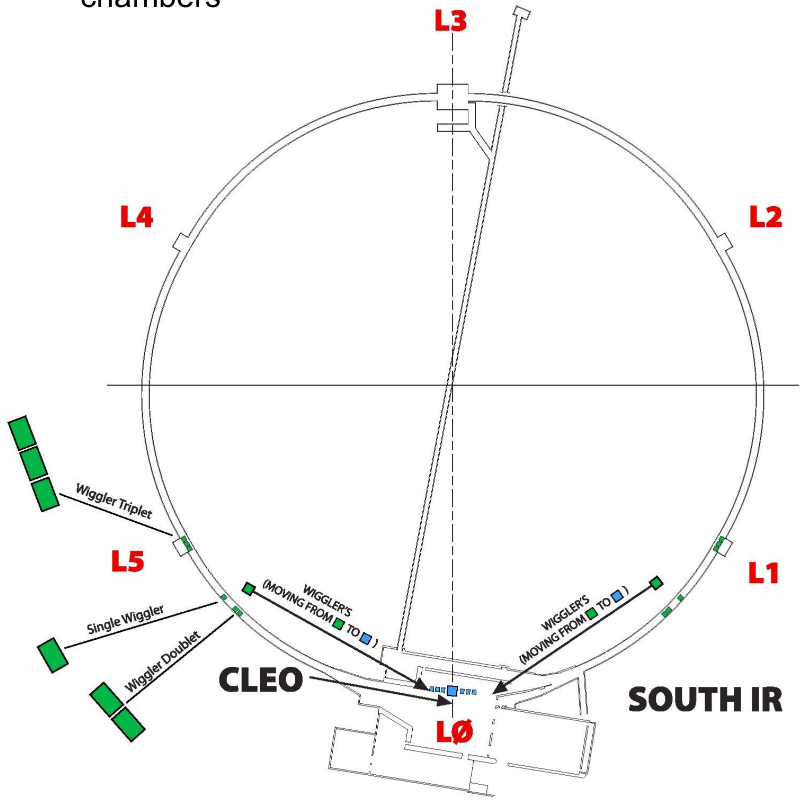

30 RFA's in drift regions, dipoles, quadrupoles, and wigglers

New electron cloud experimental regions in arcs (after 6 wigglers moved to L0 straight)

Locations for collaborator experimental vacuum chambers

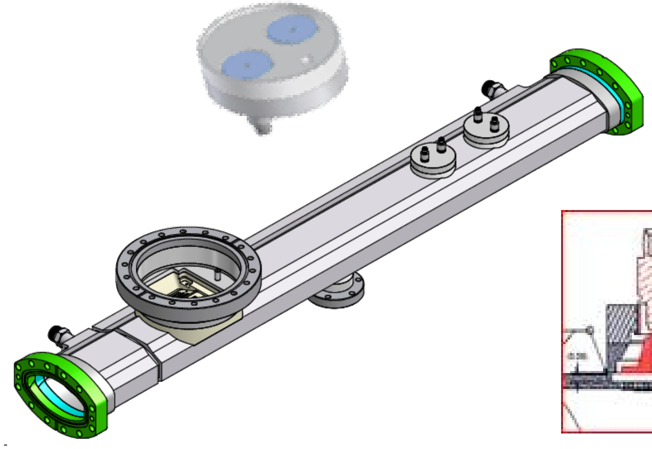

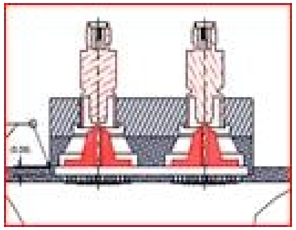

Custom vacuum chambers with shielded pickup detectors

Uncoated aluminum, and TiN, amorphous carbon, diamond-like carbon coatings

Shielded Pickup Design and Readout

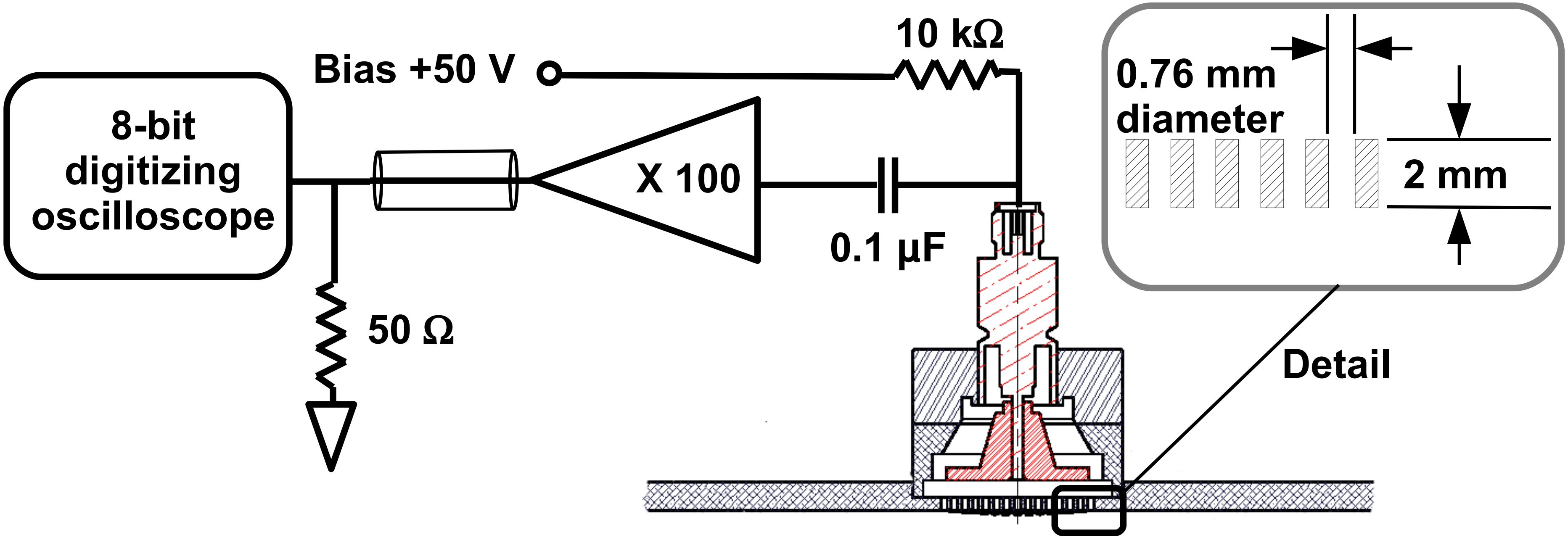

The pickup electrodes are shielded by the vacuum chamber hole pattern against the beam-induced signal.

The positive bias ensures that secondaries produced on the electrode do not escape.

Witness Bunch Method for Constraining Model Parameters Example : 5/9/2010 2.1 GeV e+ 3 mA/bunch Al v.c. 15W

Shielded pickup scope trace for two bunches 44 ns apart

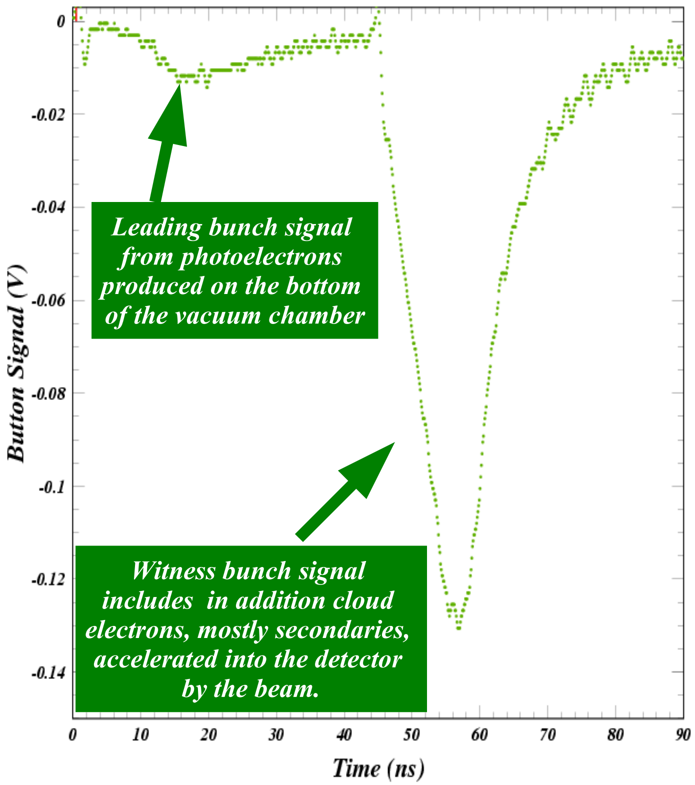

Superposition of 15 such traces illustrating the sensitivity to cloud lifetime

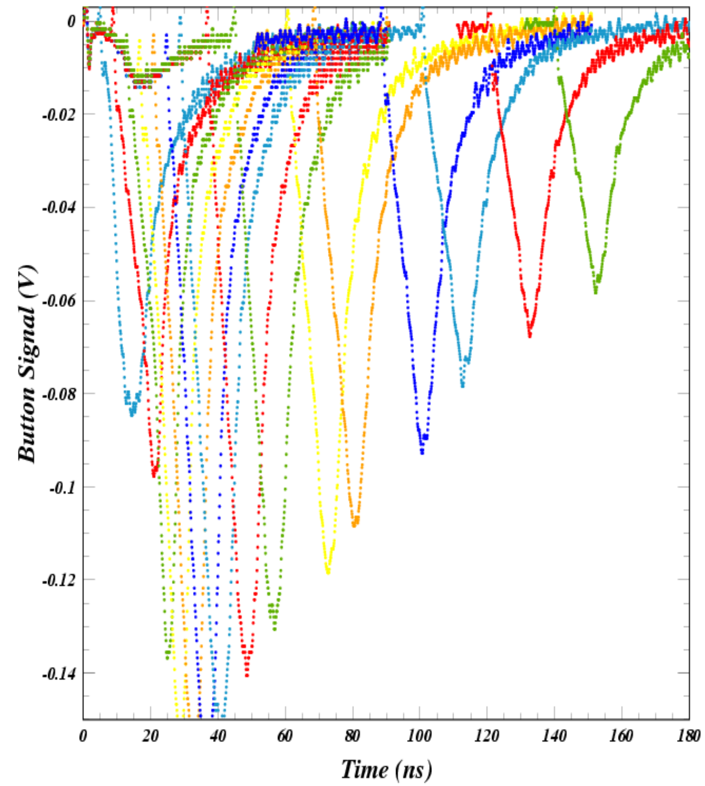

The single bunch signal arises from photoelectrons produced on the bottom of the vacuum chamber. Its shape is closely related to the photoelectron kinetic energy distribution and the beam kick. The witness bunch signal includes the single-bunch signal as well as the that produced by cloud particles accelerated into the shielded pickup by the kick from the witness bunch. The witness signal is therefore sensitive to SEY.

Electron cloud buildup modeling code ECLOUD

* Originated at CERN in the late 1990's
* Widespread application for PS, SPS, LHC, KEK, RHIC, ILC ...
* Under active development at Cornell since 2008
* Successful modeling of CESRTA tune shift measurements
* Interactive shielded pickup model implemented in 2010
* Full POSINST SEY functions added as option 2010-2012
* Flexible photoelectron energy distributions added 2011
* Synrad3D photon absorption distribution added 2011

I. Generation of photoelectrons
- A) Production energy, angle
- B) Azimuthal distribution (v.c. reflectivity)

II. Time-sliced cloud dynamics
- A) Cloud space charge force
- B) Beam kick
- C) Magnetic fields

III. Secondary yield model
- A) True secondaries (yields > 1!)
- B) Rediffused secondaries (high energy)
- C) Elastic reflection (dominates at low energy)

IV. Shielded pickup model
- A) Acceptance vs incident angle, energy
- B) Signal charge removed from cloud
- C) Non-signal charge creates secondaries

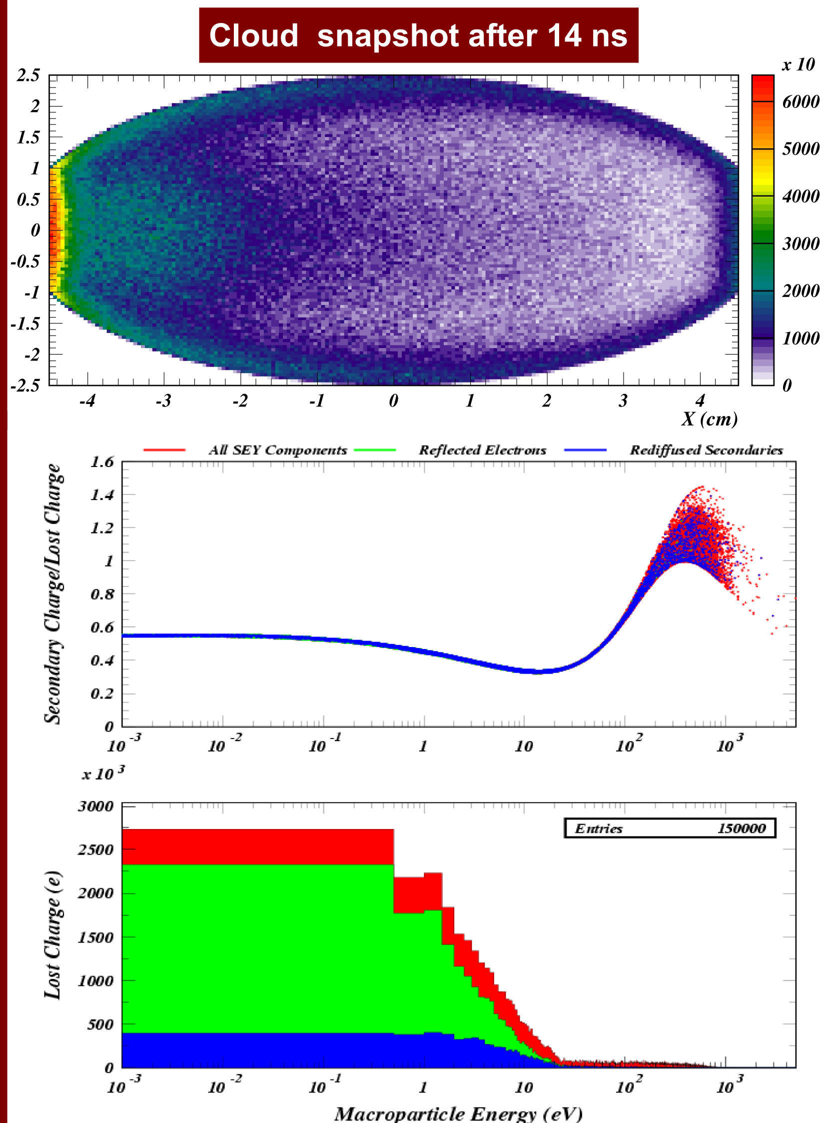

Modeled photelectron kinetic energy distribution

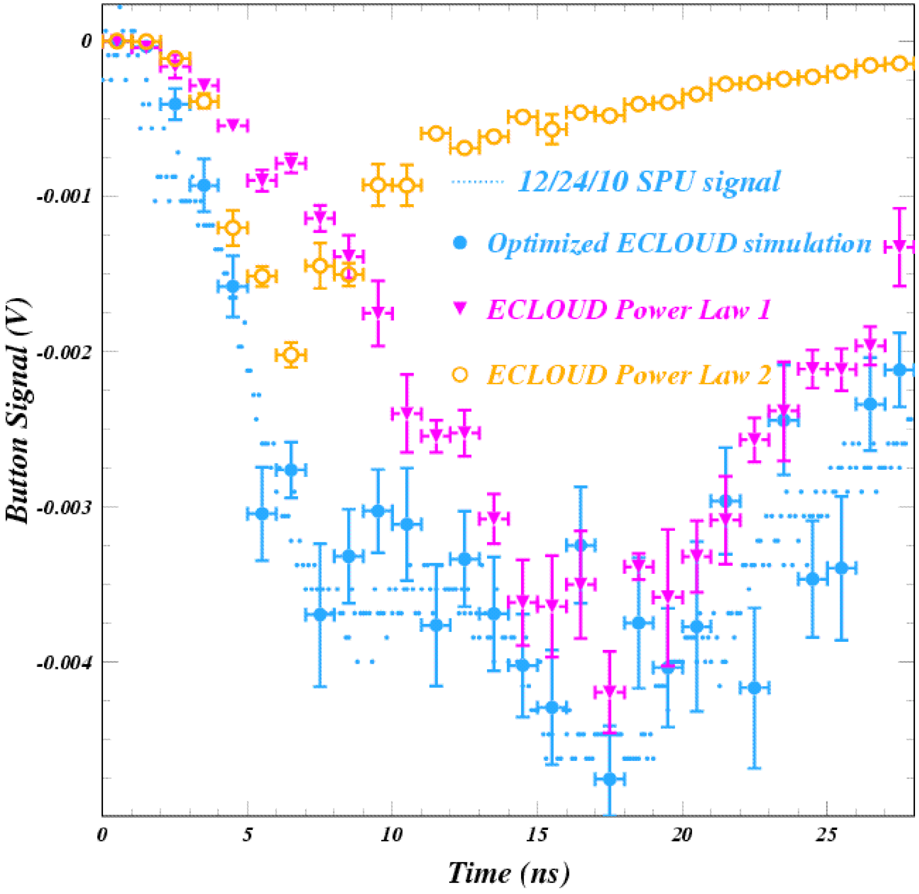

Electron Cloud Buildup Models and Plans at CESRTA
JAC et al, LCWS11

Recent Developments in Modeling Time-resolved Shielded-pickup Measurements of Electron Cloud Buildup at CESRTA
JAC et al, IPAC11

Two Power-Law Contributions

$$F(E) = E^{P1} / (1 + E/E_0)^{P2}$$

$$E_0 = E_{peak} \ (P_2 - P_1)/P_1$$

This level of modeling accuracy was achieved with the photoelectron energy distribution shown below, using a sum of two power law distributions.

$$E_{peak} = 80 \text{ eV} \quad P_1 = 4 \quad P_2 = 8.4$$

The high-energy component (22%) has a peak energy of 80 eV and an asymptotic power of 4.4. Its contribution to the signal is shown as yellow circles in the lower left plot.

$$E_{peak} = 4 \text{ eV} \quad P_1 = 4 \quad P_2 = 6$$

The low-energy component (78%) has a peak energy of 4 eV and an asymptotic power of 2. It's contribution to the signal is shown as pink triangles.

Modeled secondary electron kinetic energy distributions

Probabilistic Model for the Simulation of Secondary Electron Emission
M.A.Furman and M.F.F.Pivi, Phys. Rev. ST-AB 5, 124404 (2002)

Can Low-Energy electrons Affect High-Energy Particle Accelerators?
R.Cimino, et al, Physical Review Letters, Vol. 93, Nr. 1, 014801 (2004)

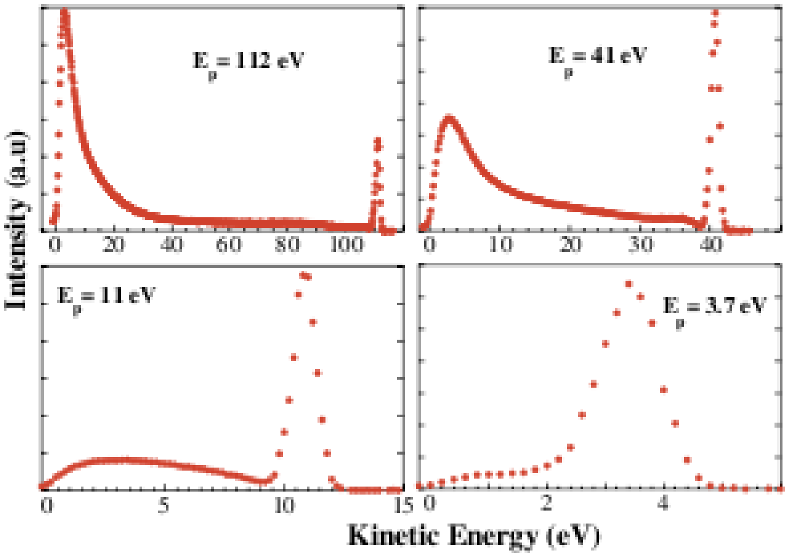

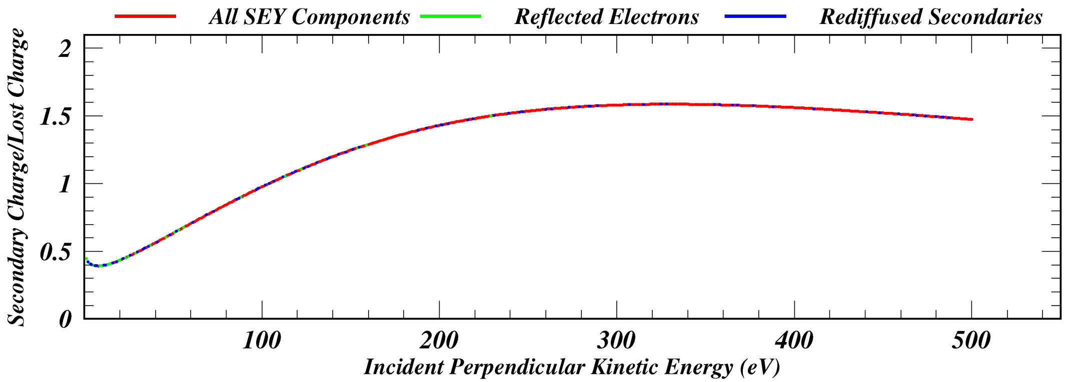

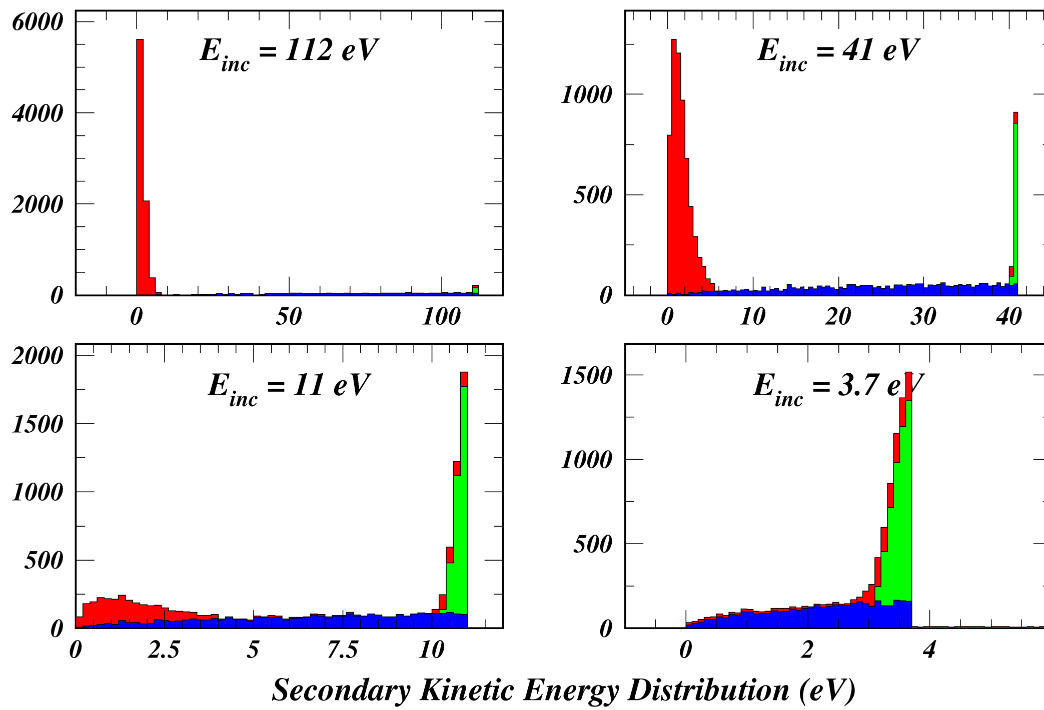

The time development of the cloud is directly dependent on secondary kinetic energies and therefore on the relative probabilities of the three secondary production processes.

Constraints on kinetic energy distribution of secondary electrons

$$f(E_{sec}) \sim E_{sec} \exp(-E_{sec}/E_{SEY})$$

Recent Developments in Modeling Time-resolved Shielded-pickup Measurements of Electron Cloud Buildup at CESRTA
JAC et al, IPAC11

Electron Cloud Buildup Models and Plans at CESRTA
JAC et al, LCWS11

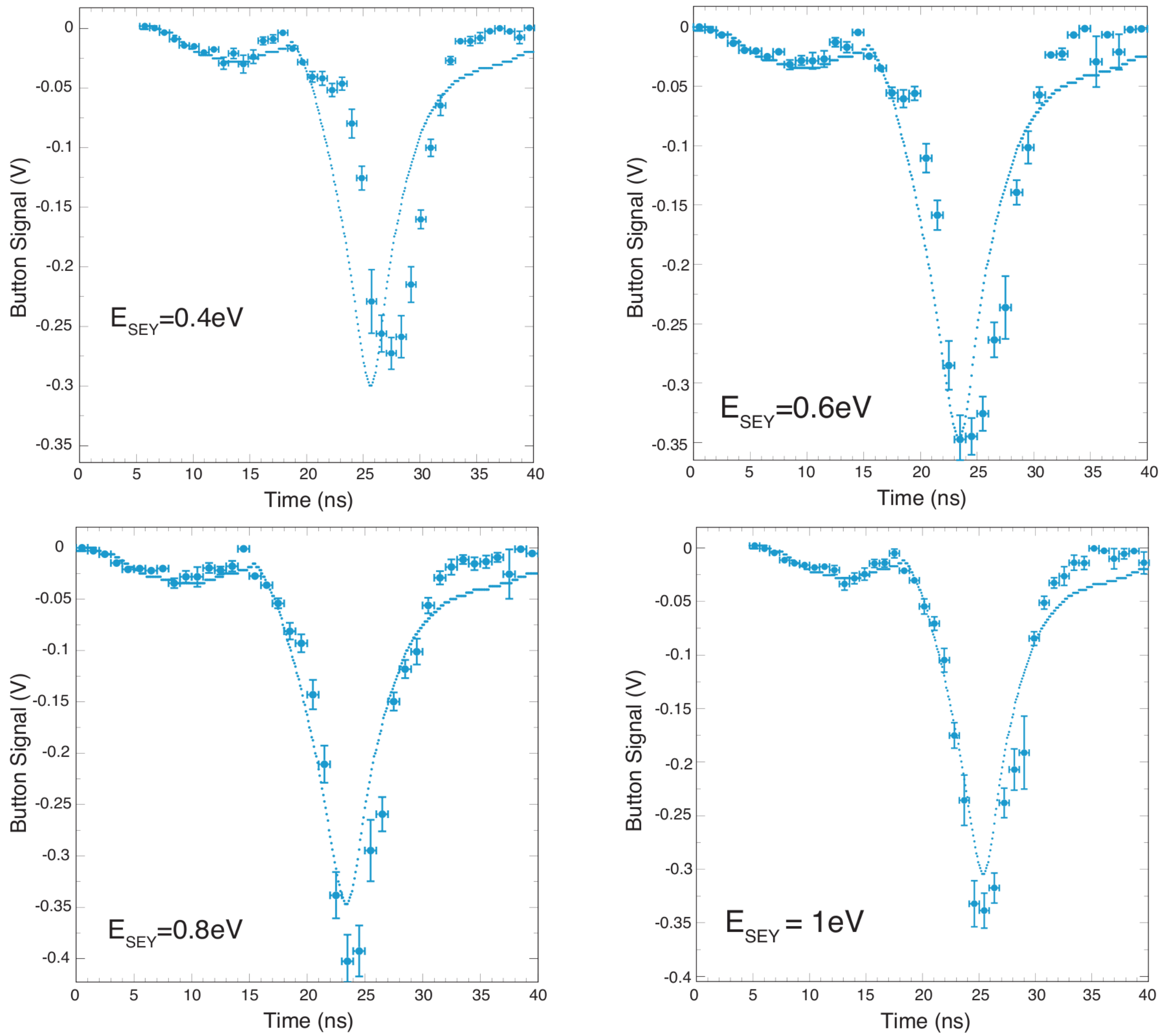

The CESRTA Test Accelerator Electron Cloud Research Program Phase 1 Report
M.A.Palmer et al, August, 2012

The pulse shape for the 14-ns witness bunch signal sets a lower bound on the model parameter E_{SEY}.

Evolution of cloud profile prior to each bunch passage

Prior to 14-ns bunch

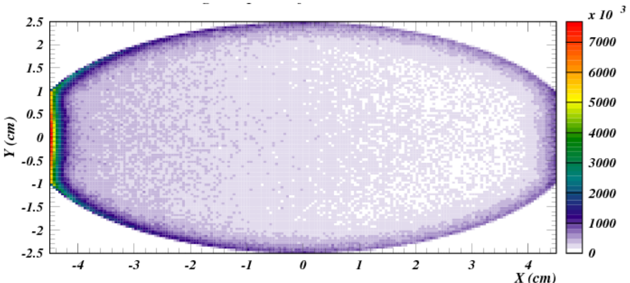

No energy cut: 1982947 macroparticles, 5.62357e+09 e-

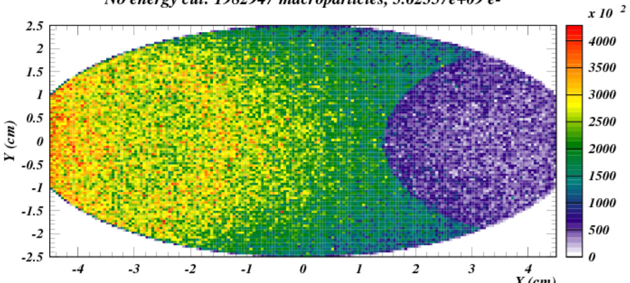

E_{kin}>10 eV: 546044 macroparticles, 2.77994e+09 e-

Prior to 28-ns bunch

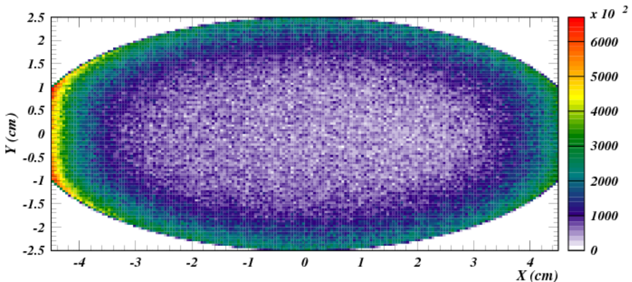

No energy cut: 1833827 macroparticles, 1879975424 e-

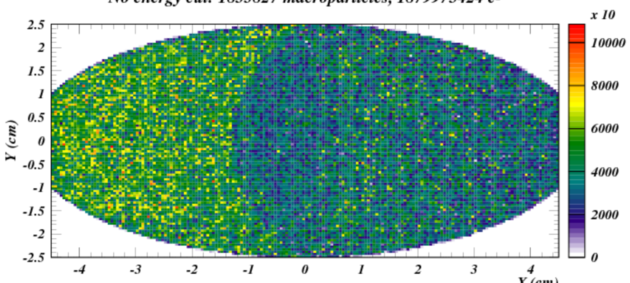

E_{kin}>10 eV: 246941 macroparticles, 599762560 e-

Prior to 84-ns bunch

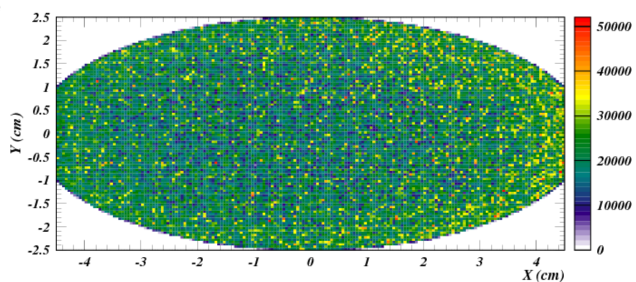

No energy cut: 1557762 macroparticles, 310677152 e-

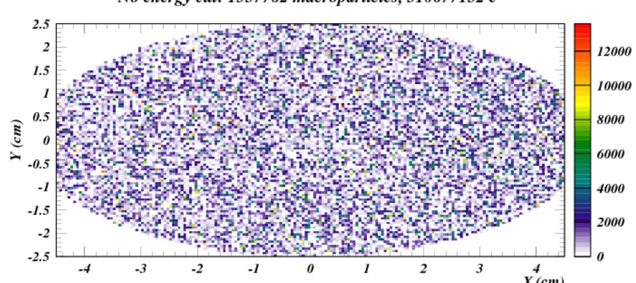

E_{kin}>10 eV: 39693 macroparticles, 16083474 e-

Determines the shielded-pickup signal shape and size.

Beam conditioning effects on an amorphous carbon coating

Recent Developments in Modeling Time-resolved Shielded-pickup Measurements of Electron Cloud Buildup at CESRTA
JAC et al, IPAC11

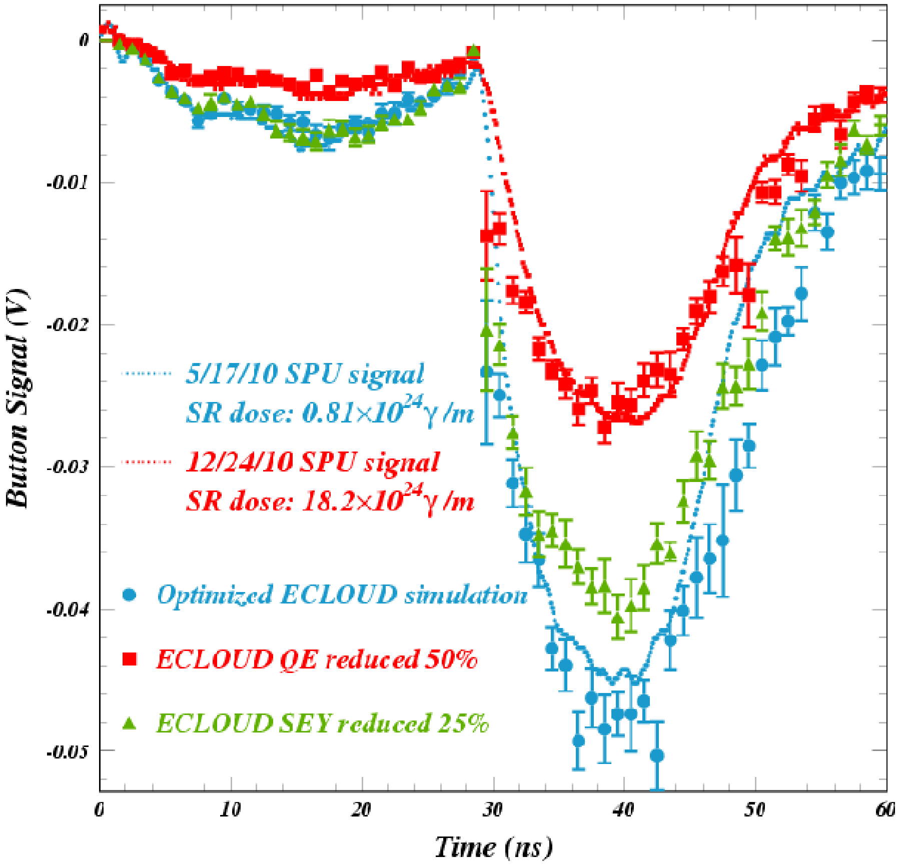

Time-resolved Shielded-pickup Measurements and Modeling of Beam Conditioning Effects on Electron Cloud Buildup at CESRTA
JAC et al, IPAC12

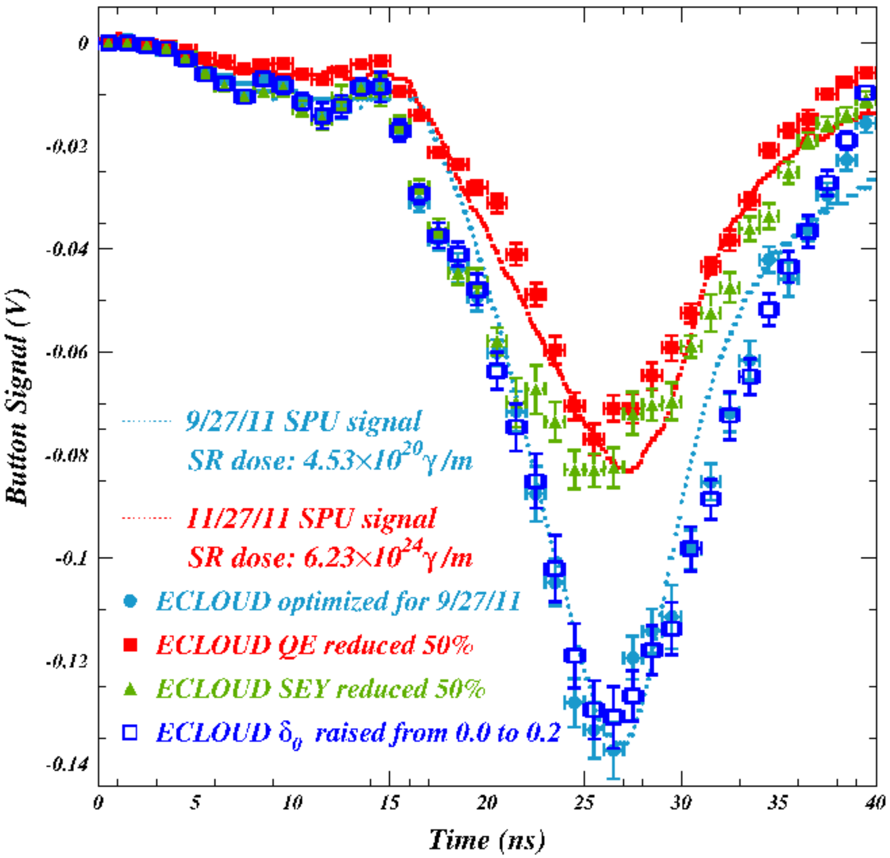

The beam conditioning effect for an amorphous carbon coating is primarily in quantum efficiency in both the early and late conditioning process.

Vacuum Chamber Comparison Under Same Beam Conditions
5.3 GeV Positron Beam
Witness bunch with 14-ns spacing

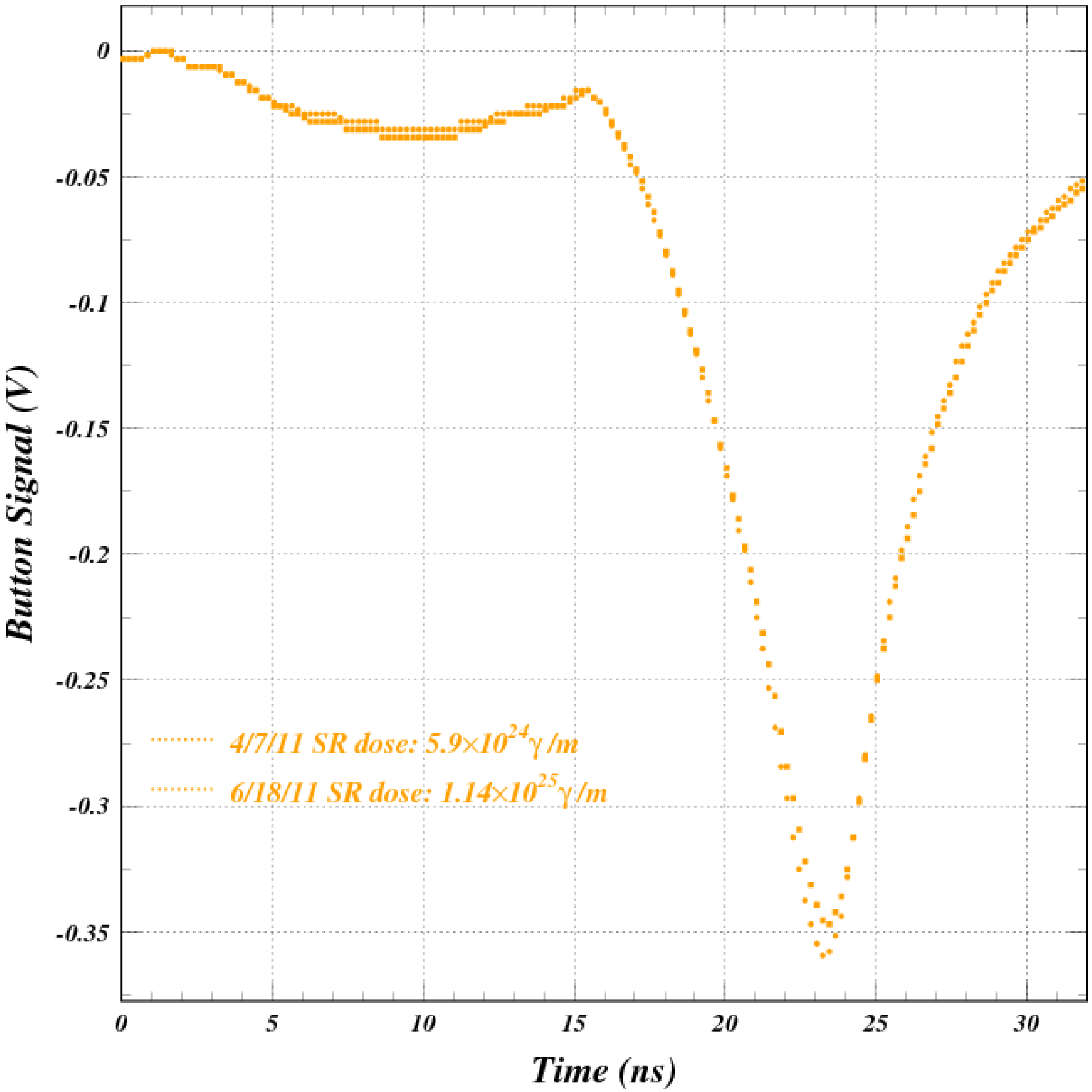

Both the quantum efficiency and secondary yield for the TiN coating is remarkably stable over this range of beam conditioning.

The reproducibility of the measurement is at the level of a few percent after two months.

Witness Bunch Study for Uncoated Aluminum 5/17/2010
15W 5.3 GeV 3 mA/bunch e+ 4-ns spacing
2010 model now updated to use Synrad3D results and vacuum chamber profile with vertical side walls

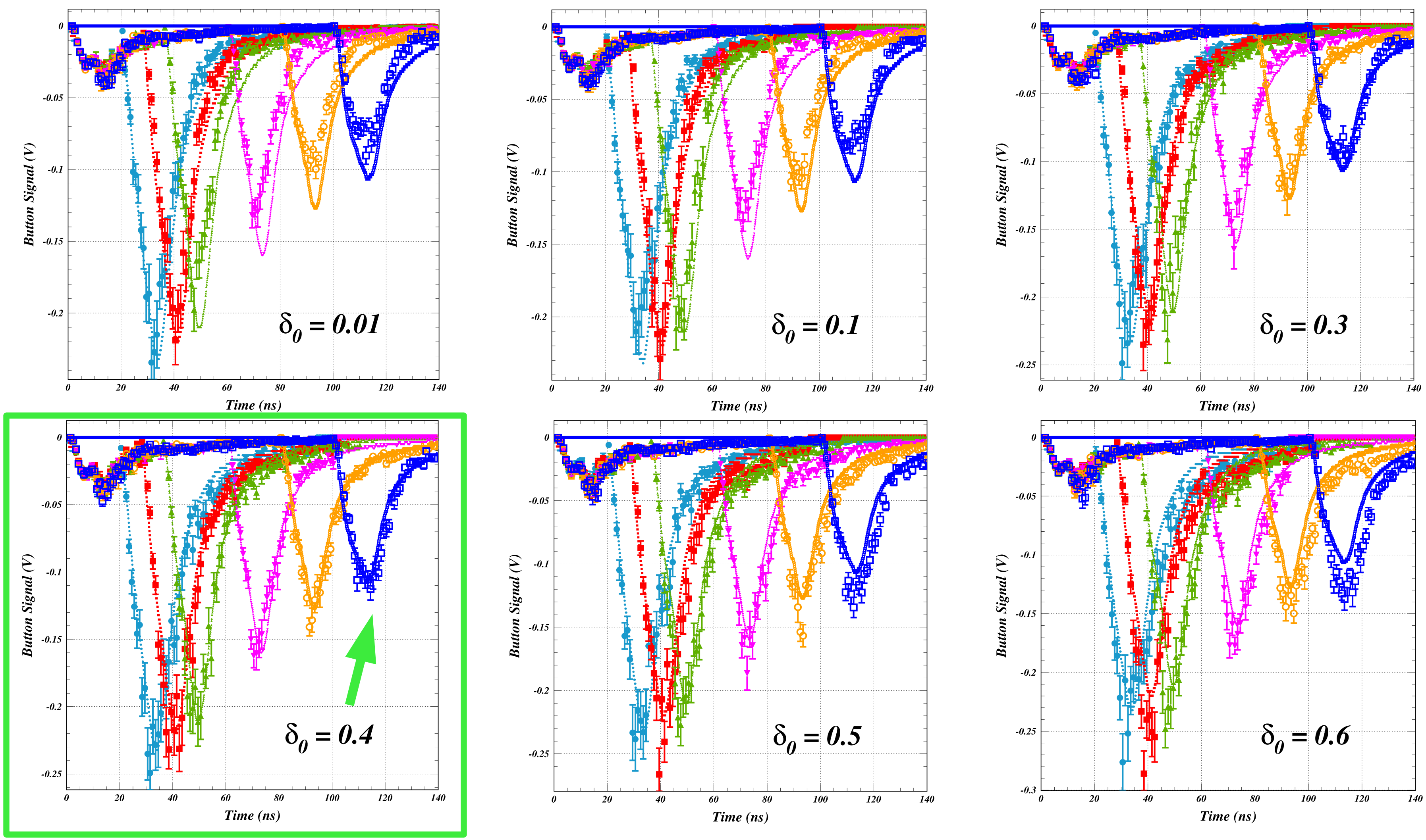

Sensitivity to value for elastic yield.

Discriminating between the true and rediffused secondary yield processes

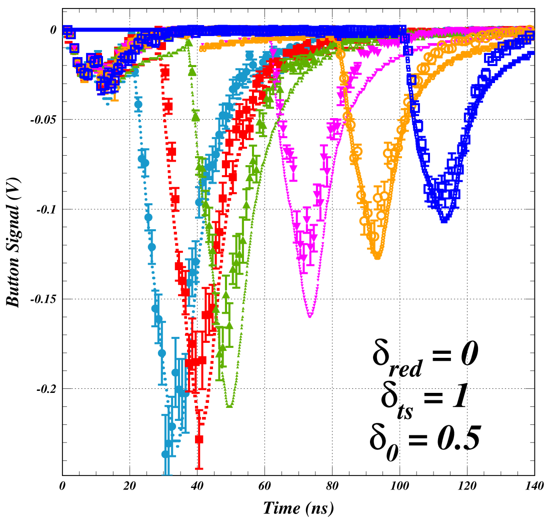

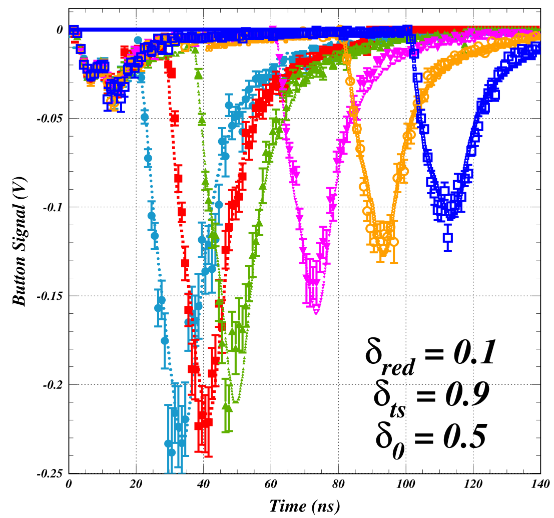

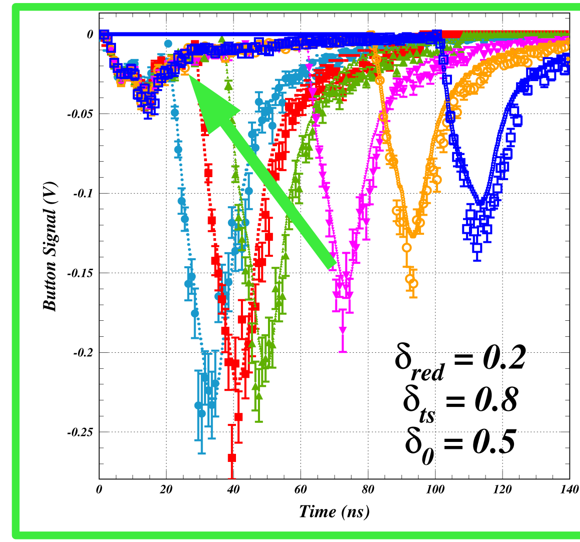

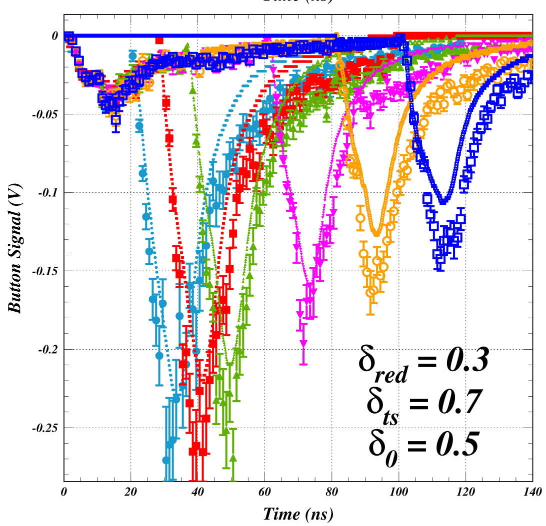

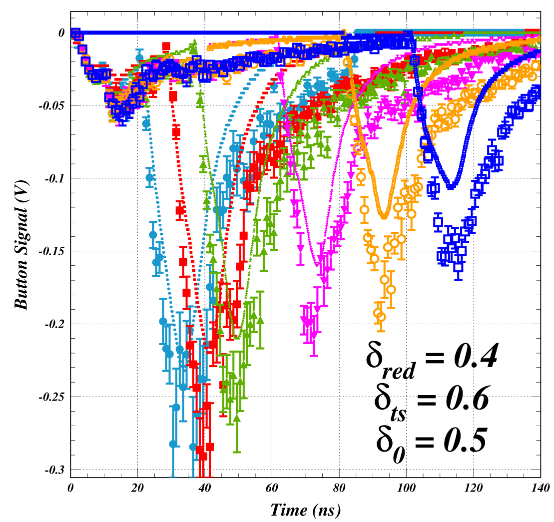

The rediffused secondary yield process determines the trailing edge of the signal from a single bunch.

This trailing edge is insensitive to δ_0.

The late witness bunch signal used to determine δ_0 is also sensitive to the rediffused yield process.

The witness bunch method provides discriminating power between the true and rediffused processes.

Witness Bunch Study for TiN-coated Aluminum
Compare today's measurements to those of 6/18/2011
15W 5.3 GeV 5 mA/bunch e+ 14-ns spacing

Present best model for 6/18/11

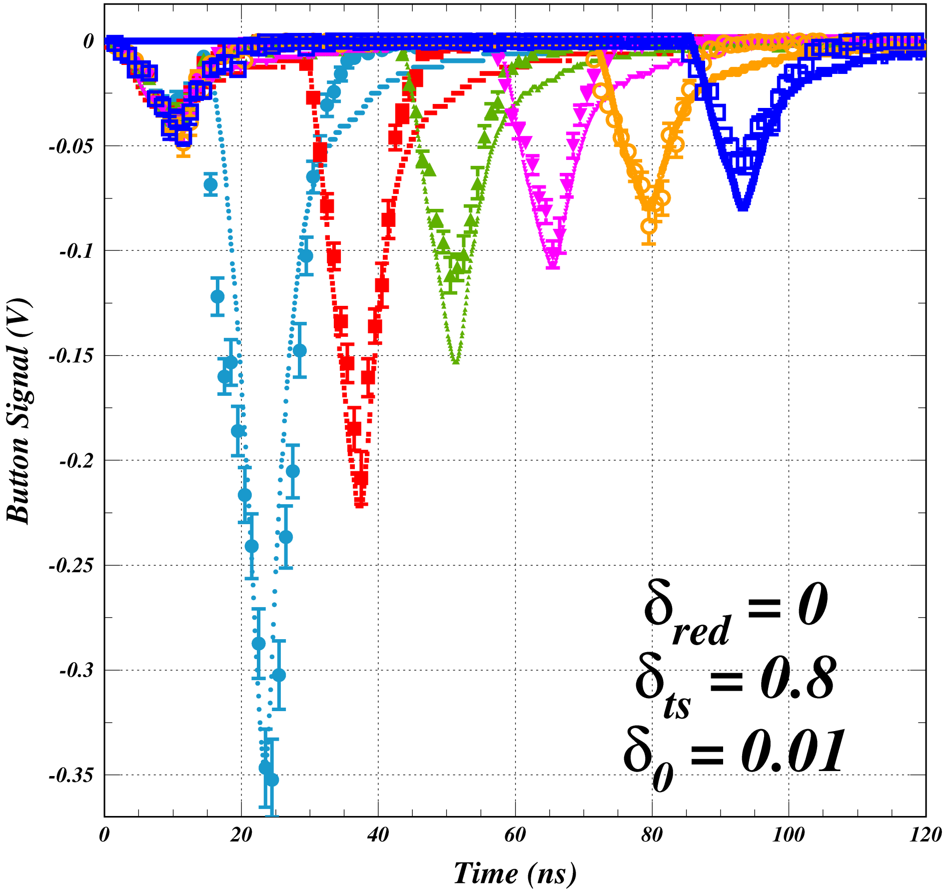

Same model with 8/22/12 measurements on unconditioned TiN

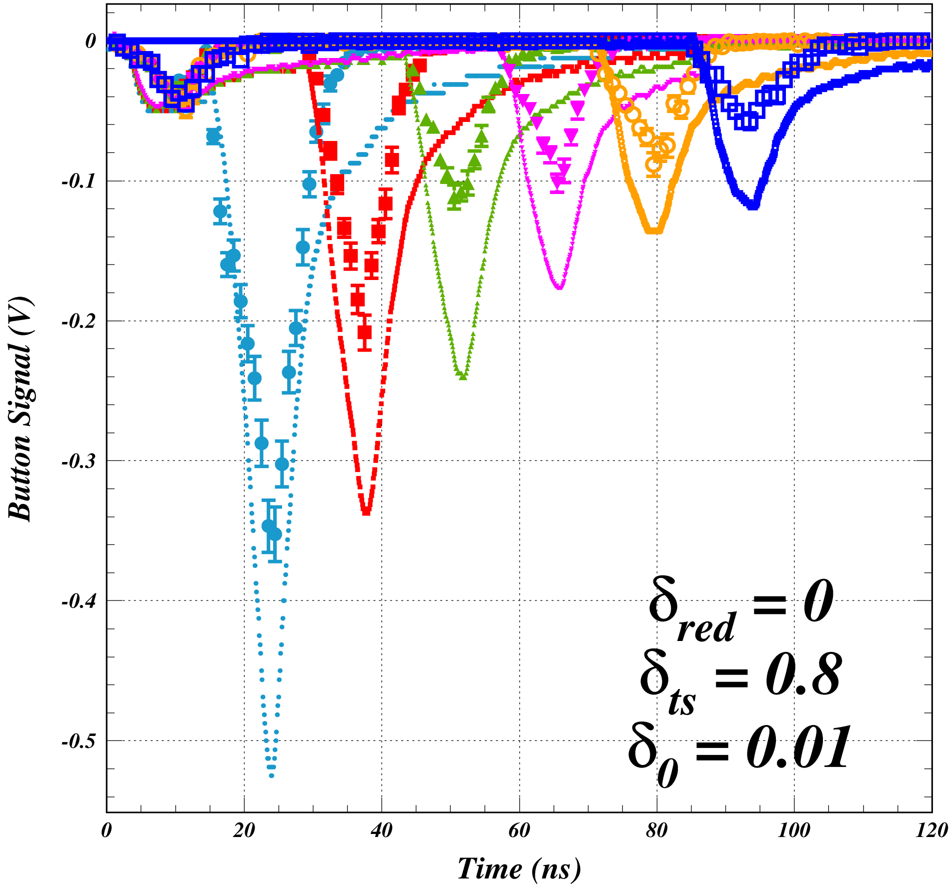

Initial indication is the the quantum efficiency is similar, but there is much more cloud due to SEY.

Witness Bunch Study for TiN-coated Aluminum
Compare recent measurements to those of 6/18/2011
15W 5.3 GeV 5 mA/bunch e+ 28-ns spacing

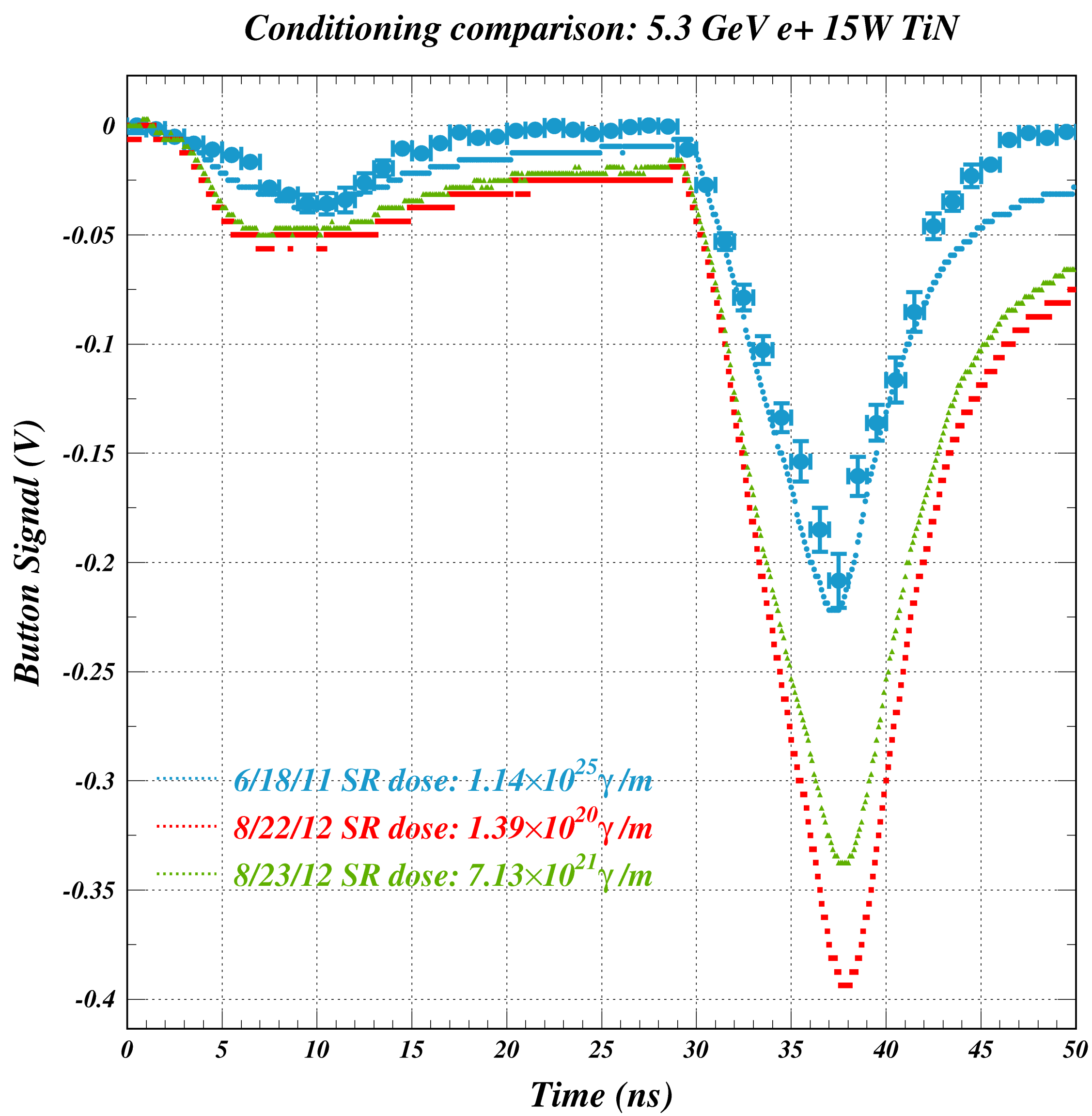

Shielded-pickup Witness Bunch Measurement Program

2010 - present

Date	Species	Beam Energy (GeV)	Bunch Current (mA)	15E/W	Mitigation Technique	Bunch Spacing (ns)
03/27/2010	Positrons	5.3	5	W	a-carbon (1)	14-84
				E	TiN	
	Electrons		5	W	a-carbon (1)	14-70
				E	TiN	
05/09/2010	Positrons	2.1	3	W	Al	4-140
				E	a-carbon (2)	
	Electrons		3	W	Al	4-20
				E	a-carbon (2)	
05/17/2010	Positrons	5.3	3	W	Al	4-100
				E	a-carbon (2)	
	Electrons		3	W	Al	4-100
				E	a-carbon (2)	
05/19/2010	Electrons	2.1	1	W	Al	4-120
				E	a-carbon (2)	
09/21/2010	Positrons	5.3	1,2,4,6,8,10	W	TiN	14
				E	a-carbon (2)	
09/24/2010	Positrons	2.1	2,4,6	W	TiN	14
				E	a-carbon (2)	
	Electrons			W	TiN	
				E	a-carbon (2)	
12/10/2010	Electrons	2.1	1,2,3,4,5,6,8,10	W	TiN	14-84
				E	a-carbon (2)	
12/20/2010	Positrons	2.1	1,2,3,4,5,6,8,10	W	TiN	56,84
				E	a-carbon (2)	
12/24/2010	Positrons	5.3	3,5	W	TiN	14-84
				E	a-carbon (2)	
	Electrons		3,5	W	TiN	14-84
				E	a-carbon (2)	
04/07/2011	Positrons	5.3	1,2,3,4,5,6,8,10	W	TiN	14-84
				E	DL carbon	
	Electrons		1,2,3,4,5,6,8,10	W	TiN	14-84
				E	DL carbon	
04/16/2011	Positrons	2.1	1,2,3,4,5,6,8,10	W	TiN	14-84
				E	DL carbon	
04/17/2011	Electrons		1,2,3,4,5,6,8,10	W	TiN	14-84
				E	DL carbon	
06/11/2011	Positrons	2.1	1,2,3,4,5,6,8,10	W	TiN	14-84
				E	DL carbon	
06/12/2011	Electrons		1,2,3,4,5,6,8,10	W	TiN	14-84
				E	DL carbon	
06/18/2011	Positrons	5.3	1,2,3,4,5,6,8,10	W	TiN	14-98
				E	DL carbon	
	Electrons		1,2,3,4,5,6,8,10	W	TiN	14-84
				E	DL carbon	
06/27/2011	Positrons	4.0	1,2,3,4,5,6,8,10	W	TiN	14-98
				E	DL carbon	
	Electrons	2.1	1,2,3,4,5,6	W	TiN	84
				E	DL carbon	
09/27/2011	Positrons	5.3	1,2,3,4,5,6,8	W	a-carbon (2)	14-84
				E	DL carbon	
09/30/2011	Positrons	5.3	1,2,3,4,5,6,8	W	a-carbon (2)	14-84
				E	DL carbon	
10/04/2011	Positrons	5.3	1,2,3,4,5,6,8	W	a-carbon (2)	14-84
				E	DL carbon	
10/11/2011	Positrons	5.3	1,2,3,4,5,6,8	W	a-carbon (2)	14-84
				E	DL carbon	
10/25/2011	Positrons	5.3	1,2,3,4,5,6,8	W	a-carbon (2)	14-84
				E	DL carbon	
11/27/2011	Positrons	5.3	1,2,3,4,5,6,8,10	W	a-carbon (2)	14-98
				E	DL carbon	
	Electrons		1,2,3,4,5,6,8,10	W	a-carbon (2)	14-84
				E	DL carbon	

2.1, 4.0, and 5.3 GeV

Electron and positron beams

1-10 mA/bunch

Uncoated aluminum
TiN-coated aluminum
Two amorphous-carbon coatings
Diamond-like carbon coating

Unconditioned uncoated aluminum
Unconditioned TiN coating
Unconditioned a-carbon coating

4-ns, 14-ns bunch spacings up to 140 ns

Vacuum Chamber Comparison Under Same Beam Conditions
5.3 GeV Positron Beam
Witness bunch with 28-ns spacing

15W | **15E**

5 mA/bunch

The a-carbon coating suppresses high-energy photoelectrons compared to the TiN coating.

The results for the second a-carbon-coated chamber corroborate the high-energy photoelectron suppression relative to TiN observed with the first a-carbon-coated chamber.

3 mA/bunch

The quantum efficiency for reflected photons and the SEY are both much smaller for the TiN coating compared to uncoated aluminum.

The second carbon-coated chamber shows conditioning effects between 5/17/10 and 12/24/10 , primarily for the quantum efficiency.